Annals of Biomedical Engineering (© 2014)
DOI: 10.1007/s10439-014-0970-3

BMES BIOMEDICAL ENGINEERING SOCIETY™ www.bmes.org

Fractional-Order Viscoelasticity in One-Dimensional Blood Flow Models

PARIS PERDIKARIS and GEORGE EM. KARNIADAKIS

Division of Applied Mathematics, Brown University, Providence, RI, USA

(*Received 15 August 2013; accepted 6 January 2014*)

Associate Editor Aleksander S. Popel oversaw the review of this article.

Abstract—In this work we employ integer- and fractional-order viscoelastic models in a one-dimensional blood flow solver, and study their behavior by presenting an *in-silico* study on a large patient-specific cranial network. The use of fractional-order models is motivated by recent experimental studies indicating that such models provide a new flexible alternative to fitting biological tissue data. This is attributed to their inherent ability to control the interplay between elastic energy storage and viscous dissipation by tuning a single parameter, the fractional order α, as well as to account for a continuous viscoelastic relaxation spectrum. We perform simulations using four viscoelastic parameter data-sets aiming to compare different viscoelastic models and highlight the important role played by the fractional order. Moreover, we carry out a detailed global stochastic sensitivity analysis study to quantify uncertainties of the input parameters that define each wall model. Our results confirm that the effect of fractional models on hemodynamics is primarily controlled by the fractional order, which affects pressure wave propagation by introducing viscoelastic dissipation in the system.

Keywords—1D blood flow, Viscoelasticity, Fractional-order constitutive laws, Global stochastic sensitivity.

INTRODUCTION

The vascular wall is a heterogeneous soft tissue with complex bio-mechanical properties that vary over different locations in the arterial tree and the temporal state of the response (deformation/relaxation). It is comprised of three different layers: the intima (mainly endothelial cells), the media (mainly smooth muscle cells), and the adventitia (mainly collagenous fibers).[12] This structure highlights two key functions, namely, reversible energy storage (elasticity) and energy dissipation (viscosity).

Address correspondence to George Em. Karniadakis, Division of Applied Mathematics, Brown University, Providence, RI, USA. Electronic mail: paris_perdikaris@brown.edu, george_karniadakis@brown.edu

Constitutive laws for biological tissue can be derived using integer-order differential equations that model stress–strain relations using additive combinations of purely elastic and viscous elements.[12] The simplest integer-order models of linear viscoelasticity are the Voigt and standard linear solid (SLS or Kelvin–Zener) models.[10] The Voigt model can be constructed by the parallel combination of a spring and a dashpot and it is the simplest model that accounts for creep and hysteresis phenomena. Similarly, the SLS model is constructed using the parallel combination of a spring with a spring and a dashpot in series, and it accounts for creep, hysteresis and stress relaxation phenomena.

Due to their simplicity, these models have been used in several 1D blood flow studies to describe arterial wall viscoelasticity.[1,4,8,22,23,28] In Alastruey *et al.*,[1] a 1D model employing a Voigt viscoelastic model is assessed in comparison with *in vitro* measurements of flow in 37 silicone branches representing the largest central systemic arteries in the human. In Reymond *et al.*,[23] a more generalized integer-order viscoelastic model is considered, and 1D simulations are compared against *in vivo* measurements in a patient-specific network of 94 large systemic arteries. Both studies show good agreement between simulations and measured data, indicating that 1D models may capture the most significant features of the pulsatile flow and pressure waveforms. However, they mainly focus on larger systemic arteries, where the arterial wall response is known to be predominantly elastic,[5,6] whereas the effect of wall viscoelasticity on hemodynamics is minor and only manifested in distal locations,[23] where the arterial wall appears to be more muscular.

Fung's quasi-linear viscoelasticity (QLV) theory[12] provides a path to constructing integer-order models that accurately capture the time-depended response of the arterial wall; however, estimating the elastic and viscoelastic parameters that define these models in different anatomic locations still remains a very chal-

Published online: 11 January 2014

lenging task. In particular, one needs to address the lack of clinical data, the local and patient-specific nature of parameter values, the dynamic variation that parameters such as the Young's modulus E may exhibit during the cardiac cycle, *etc*. Also, as reported in Doehring *et al*.,[9] the sensitivity on these parameters (especially the long viscoelastic relaxation time) is high. These are key limiting factors for considering integer-order QLV models in 1D blood flow simulations of large arterial networks with high spatial variability in mechanical properties and presence of regions where the viscoelastic response of the wall may be significant.

An alternative approach to modeling the viscoelastic behavior of arteries based on *fractional calculus*[17,18,20] has been introduced in Craiem and Armentano,[5] Craiem *et al*.,[6] and Doehring *et al*.,[9] where the cell and tissue biomechanics are modeled by *fractional-order* differential equations. Under this framework, a spring represents a zero-order element (purely elastic response) and a dashpot corresponds to a first-order element (purely viscous response). A fractional order $0 < \alpha < 1$ results in a new flexible element type, the so-called *spring-pot*,[17] which essentially interpolates between the purely elastic and viscous behaviors and can be thought of as a large set of weighted integer-order spring/dashpot pairs arranged in parallel.[19] This gives rise to a very interesting physical interpretation: the fractional order introduces a fractal tree-like hierarchical structure, naturally allowing for separation of material and global time scales (see Doehring *et al*.,[9] Fig. 1). In contrast to the discrete relaxation spectrum of linear Voigt and SLS integer-order models, fractional-order models exhibit a continuous relaxation distribution, spanning all frequencies above zero, up to infinity. Therefore, fractional-order models can be naturally put under the context of QLV and be considered as good candidates for modeling biological tissue, which in reality shows continuous relaxation.[12]

Recent experimental studies have confirmed the ability of fractional-order models to capture the dynamic response of the vascular wall. Specifically, in Craiem and Armentano[5] the authors proposed a fractional-order Voigt model (FO-Voigt) and accurately described the viscoelastic mechanical response of the aorta of a sheep *in-vivo* with a minimal set of estimated parameters. Also, in Craiem *et al*.,[6] uniaxial loading experiments were performed to strips cut from healthy human aortas, and a FO-Voigt model was successfully fitted to measured stress–relaxation data. Similarly, in Craiem *et al*.,[7] FO-Voigt and fractional-order SLS (FO-SLS) models were calibrated to accurately reproduce *in-vivo* data from ascending aorta segments of four human donors. In Doehring *et al*.,[9] a fractional stress relaxation function corresponding to a FO-SLS model was integrated in the QLV framework to successfully model aortic valve cusp biomechanics, while demonstrating significantly lower sensitivity on the input parameters as compared to a standard QLV model with a continuous relaxation spectrum. These recent findings indicate that fractional order models may offer a new powerful alternative for describing arterial wall mechanics, reducing the parameter estimation count and overcoming the sensitivity limitations of integer-calculus-based QLV models.

In this paper, we present a nonlinear, time-domain 1D blood flow formulation integrated with integer- and fractional-order viscoelastic wall models. We perform blood flow simulations in a large patient-specific network and compare integer- and fractional-order SLS models, calibrated with experimental data reported in the literature. Our main scientific goal is to quantify the effect of the fractional-order and the viscoelastic relaxation response on the computed flow and pressure wave propagation. Finally, we present a global sensitivity analysis study for which we have considered a stochastic fractional-order SLS model by introducing uncertainty in the parameters that define its viscoelastic behavior.

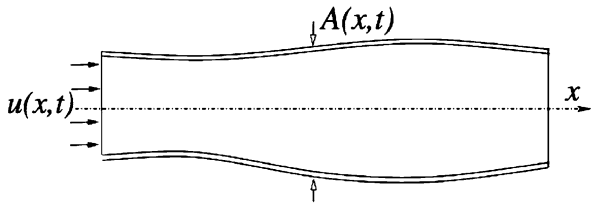

FIGURE 1. Flow in a 1D compliant tube (from Sherwin *et al*.[25]).

METHODS

The derivation of a model describing viscous 1D incompressible flow in a compliant tube is based on the assumptions of axial symmetry, dominance of the axial velocity component, radial displacements of the arterial wall, and constant internal pressure on each cross section (see Fig. 1). This formulation leads to a nonlinear hyperbolic system of equations that yields conservation of mass and momentum in space–time (A, U) variables (for a detailed analysis see Formaggia *et al*.[11] and Sherwin *et al*.[25])

$$\begin{cases} \frac{\partial A}{\partial t} + \frac{\partial (AU)}{\partial x} = 0 \\ \frac{\partial U}{\partial t} + U\frac{\partial U}{\partial x} = -\frac{1}{\rho}\frac{\partial p}{\partial x} + K_r \frac{U}{\rho A}, \end{cases} \quad (1)$$

where x is the axial coordinate across the vessel's length, t is time, $A(x, t)$ is the cross-sectional area of the lumen, $U(x, t)$ is average axial fluid velocity,

$Q(x, t) = AU$ is the mass flux, $p(x, t)$ is the internal pressure averaged over the tube's cross-section, $K_r = -22\mu\pi$ is a friction parameter that depends on the velocity profile chosen,[27] and μ is the blood viscosity. Here, we assume a constant blood viscosity since Non-Newtonian effects are known to be minor in larger systemic arteries.[11,24] Introducing a profile that satisfies the no-slip condition we can recover the axisymmetric fluid velocity $u(x, r, t)$

$$u(x,r,t) = U\frac{\zeta+2}{\zeta}\left\{1-\left(\frac{r}{R}\right)^{\zeta}\right\}, \tag{2}$$

where, $R(x, t)$ is the lumen radius, ζ is a constant, and r is the radial coordinate. Following Smith *et al.*,[27] $\zeta = 2$ returns the standard Poiseuille flow profile, while $\zeta = 9$ gives a good fit to experimental blood flow data.

In order to solve Eq. (1) for (A, U), we need to provide a pressure–area relation.[11,25] The most basic and popular choice is based on the purely elastic tube law, in which stress σ and strain ε are related as

$$\sigma(t) = E\epsilon(t), \tag{3}$$

where,

$$\sigma = \frac{r(p-p_{\text{ext}})}{h} \quad \text{and} \quad \epsilon = \frac{1}{1-\nu^2}\frac{r-r_0}{r_0} \tag{4}$$

Here, p_{ext} is the external pressure on the arterial wall, E is the Young modulus of the wall, h is the wall thickness, ν is the Poisson ratio, and r_0 is the lumen radius corresponding to a reference cross-sectional area $A_0 = \pi r_0^2$ at equilibrium state $(p, U, A) = (p_{\text{ext}}, 0, A_0)$.

Substituting Eq. (4) in Eq. (3) we arrive at the purely elastic pressure–area relation

$$p = p_{\text{ext}} + \beta(\sqrt{A} - \sqrt{A_0}), \tag{5}$$

where β is defined assuming that $\frac{1}{\sqrt{A}}$ can be approximated by $\frac{1}{\sqrt{A_0}}$.

$$\beta = \frac{\sqrt{\pi}Eh}{(1-\nu^2)A_0} \tag{6}$$

While one can employ more realistic nonlinear elastic stress–strain laws,[29] in this study we aim to study the sensitivity of the flow with respect to viscoelasticity. To this end, we choose to model elastic behavior using the simple elastic tube law of Eq. (5) that has been extensively used in the literature.[1,11,13,25]

Viscoelastic Models of the Arterial Wall

Fung's QLV theory[12] provides a unifying framework under which general soft tissue constitutive laws can be formulated. Such models are often characterized by a constant hysteresis over a wider frequency range. Based on this approach we have a stress–strain relation of the form

$$\sigma(x,t) = \int_0^{\infty} G(t-\gamma)\frac{\partial \epsilon^{\text{e}}(x,\gamma)}{\partial \gamma}d\gamma, \tag{7}$$

where $G(t)$ is the stress relaxation function and $\varepsilon^{\text{e}}(x, t)$ is the static elastic response of the tissue. The presence of the convolution integral in Eq. (7) makes the stress depend upon the strain time history, but it is the choice of the stress relaxation function that ultimately determines the tissue model. Typically, one introduces a parametric representation of $G(t)$ that fits given experimental measurements.[28,29] In the following sections we present the fractional-order SLS model and its implementation in a one-dimensional blood flow solver.

The Fractional SLS Model (Fractional Kelvin–Zener Model)

Before we present the fractional version of the SLS model, we start with the classical definition of the Caputo fractional derivative of order α[18]

$${}_0^C D_t^{\alpha} f(t) := \begin{cases} \frac{1}{\Gamma(n-\alpha)}\int_0^t \frac{f^{(n)}(\tau)}{(t-\tau)^{\alpha+1-n}}d\tau, & n-1<\alpha<n \\ \frac{d^n f(t)}{dt^n}, & \alpha = n \end{cases}, \tag{8}$$

where $\alpha > 0$ is a real number, n is an integer, and $\Gamma(\cdot)$ is the Euler gamma function. We note that for $\alpha \neq n$, the Caputo derivative is a non-local operator that depends on the history of f in the interval $[0,t]$.

The fractional order generalization of the SLS model is constructed using the parallel combination of a spring with a spring in series with a *spring-pot*. The stress is related to strain as

$$\sigma(t) + \tau_{\sigma 0}^{\alpha}{}^C D_t^{\alpha}\sigma(t) = E\left[\epsilon(t) + \tau_{\epsilon 0}^{\alpha}{}^C D_t^{\alpha}\epsilon(t)\right] \tag{9}$$

We observe that simpler fractional- and integer-order viscoelastic models as well as the purely elastic tube law appear as limiting cases in the above equation. Namely, for $\alpha = 1$, we recover the classic integer-order SLS model, while taking $\tau_{\sigma} = 0$ results to the fractional-order Voigt model.

Thermodynamic consistency of the FO-SLS model requires a monotonically decreasing stress relaxation function, which further implies that the fractional time derivatives of both the stress and the strain must be of the same order α.[2,19]

By employing the Laplace transform, we can express the FO-SLS stress relaxation function as

$$G(t) = E\left(\frac{\tau_\epsilon}{\tau_\sigma}\right)^\alpha + E\left(\left[\frac{\tau_\epsilon}{\tau_\sigma}\right]^\alpha - 1\right) E_{\alpha,1}\left(-\left[\frac{t}{\tau_\sigma}\right]^\alpha\right), \quad (10)$$

where $E_{\alpha,\beta}(t)$ is the two parameter Mittag-Leffler function, known as the fractional generalization of the exponential

$$E_{\alpha,\beta}(t) := \sum_{n=0}^{\infty} \frac{t^n}{\Gamma(\alpha - n\beta)} \quad (11)$$

Compared to the standard exponential function, the Mittag-Leffler function exhibits very different behavior[18]: for small times it exhibits a much faster decay than the exponential, while at the limit $t \to \infty$ the decay is only algebraic. This heavy tail decay is what characterizes the Mittag-Leffler function as a *super-slow process*.[18]

Another important observation here is that for the FO-SLS model the idea of relaxation times must be revised. Under the fractional setting, they no longer represent single discrete relaxation frequencies but they should be rather be interpreted as break-frequencies in a Cole–Cole model sense, around which the model characteristics change.[19]

Finally, by substituting the FO-SLS stress relaxation function of Eq. (10) in Eq. (7), integrating by parts and employing the definitions in Eq. (4) we arrive at the FO-SLS pressure–area relation

$$p(x,t) = p_{\text{ext}} + p^{\text{E}}(x,t) + p^{\text{V}}(x,t), \quad (12)$$

where p^{E}, p^{V} correspond to the elastic and viscoelastic pressure contributions, respectively.

$$p^{\text{E}}(x,t) = \left(\frac{\tau_\epsilon}{\tau_\sigma}\right)^\alpha \beta(\sqrt{A} - \sqrt{A_0})$$

$$p^{\text{V}}(x,t) = \frac{1}{\tau_\sigma}\left(1 - \left[\frac{\tau_\epsilon}{\tau_\sigma}\right]^\alpha\right) \int_0^t E_{\alpha,0}\left(-\left[\frac{t-\gamma}{\tau_\sigma}\right]^\alpha\right) p^{\text{E}}(\gamma) d\gamma \quad (13)$$

We observe that the FO-SLS model introduces stress–strain memory effects that in the long time limit decay algebraically due to the Mittag-Leffler relaxation kernel.[18] It is important to note here that thanks to the linearity of the time-fractional ODE governing the fractional-order SLS model (Eq. (9)), the Laplace transform allows us to arrive to Eq. (12), which corresponds to the exact solution of Eq. (9).

An alternative way of formulating the required pressure–area relation arises from directly discretizing the Caputo time derivatives in the fractional constitute law that defines each model using an appropriate discretization technique. The easiest and most popular way of doing this is by employing the Grünwald–Letnikov formula[20]:

$$\begin{aligned} {}_0^C D_t^\alpha f(t) &= \lim_{\Delta t \to 0} \Delta t^{-\alpha} \sum_{k=0}^{\infty} GL_k^\alpha f(t - k\Delta t), \\ GL_k^\alpha &:= \frac{k - \alpha - 1}{k} GL_{k-1}^\alpha, \end{aligned} \quad (14)$$

with $GL_0^\alpha = 1$. By substituting the Grünwald–Letnikov formula in Eq. (9), we can formulate the pressure–area relation for the FO-SLS model as

$$\begin{aligned} p(x,t) = p_{\text{ext}} + \frac{1 + \tau_\epsilon^\alpha \Delta t^{-\alpha}}{1 + \tau_\sigma^\alpha \Delta t^{-\alpha}} p^{\text{E}}(x,t) + \frac{\Delta t^{-\alpha}}{1 + \tau_\sigma^\alpha \Delta t^{-\alpha}} \\ \times \sum_{k=0}^{\infty} GL_k^\alpha \left\{ \tau_\epsilon^\alpha p^{\text{E}}(t - k\Delta t) - \tau_\sigma^\alpha p(t - k\Delta t) \right\}, \end{aligned} \quad (15)$$

where the last term in the summation is the total elastic and viscoelastic pressure from previous time steps.

An attractive feature of this approach is that for a small time step Δt, which is typically the case for the high-order polynomial approximations employed here (due to the Courant–Friedrichs–Lewy (CFL) condition), the Grünwald–Letnikov coefficients exhibit fast decay properties. This enables us to reduce the computation of the convolution sum in Eq. (15), by using a "short memory" principle,[20] and approximate the viscoelastic memory effects using only a portion of the response history, disregarding any terms in the Grünwald–Letnikov expansion that are below a cutoff threshold. However, the elastic behavior of larger systemic arteries typically corresponds to low values of the fractional order,[5,6] and the accurate evaluation of these convolutions using the "short memory" principle requires one to consider history effects from the last four cardiac cycles. Our numerical experiments indicate that this is the minimum amount of time-history required by the Grünwald–Letnikov formula to give numerically stable and convergent results for the problem considered. With our goal being the long-time integration of Eq. (1), using a time step as low as $\Delta t = 10^{-6}$, and with each cardiac cycle being about 1 s long, this results to storing at least 4×10^6 values per history point. This value, in combination with the requirement to compute a convolution sum at each quadrature point and for each time step, renders the simulation completely *unrealistic* even on modern supercomputers. In "Evaluation of Hereditary Integrals" section, we will present a formulation that alleviates the computational complexity introduced by fractionality, and finally arrive at a computable workflow that employs the exact solution of Eq. (9) and accounts for the full time history in the evaluation of hereditary integrals.

Numerical Method

The system of is hyperbolic and can be discretized in space using the Discontinuous Galerkin method.[25] Here, we present a brief outline of the numerical method first introduced in Sherwin *et al.*[25] The system of Eq. (1) can be written in conservative form as

$$\frac{\partial \mathbf{U}}{\partial t}+\frac{\partial \mathbf{F}(\mathbf{U})}{\partial x}=\mathbf{S}(\mathbf{U}),\quad \mathbf{U}=\begin{bmatrix}A\\U\end{bmatrix},$$
$$\mathbf{F}=\begin{bmatrix}AU\\ \frac{U^2}{2}+\frac{p^{\mathrm{E}}}{\rho}\end{bmatrix}+\begin{bmatrix}0\\ \frac{p^{\mathrm{V}}}{\rho}\end{bmatrix},\quad \mathbf{S}(\mathbf{U})=\begin{bmatrix}0\\ -22\mu\pi\frac{U}{\rho A}\end{bmatrix} \tag{16}$$

The computational domain Ω consists of arterial segments, which can be divided in *Nel* elemental non-overlapping regions $\Omega_e=(x_e^L,x_e^R)$, such that $x_e^R=x_{e+1}^L$ for $e=1,\ldots,Nel$. The solution in each element is approximated by an expansion of orthogonal Legendre polynomials. Under the Discontinuous Galerkin formulation, the solution may be discontinuous across elemental interfaces, with global continuity being recovered by solving a Riemann problem for the upwinded flux $\mathbf{F}$ that propagates information between the elemental regions and the bifurcations of the system. At the inlet and outlet boundary elements, the fluxes are upwinded by means of the boundary conditions; the hyperbolic nature of the system requires only one boundary condition at each terminal end. Finally, time-integration is performed using a standard second-order accurate Adams–Bashforth scheme.[25]

At bifurcation and junction points of the network we require continuity of the characteristics (Riemann invariants), conservation of mass and continuity of total pressure (see Sherwin *et al.*[25] for a detailed analysis). Terminal vessels are typically coupled to 0D lumped parameter models. Here we employ a 3-parameter Windkessel model, in which we need to *a-priori* specify the total peripheral resistance downstream of the outlet R_t, and a corresponding compliance C, based on parameter estimation or clinical measurements.[11]

It is important to note that viscoelasticity adds dissipation, leading to a system that is no longer strictly hyperbolic. However, the conservative elastic contribution is still dominant, thus allowing us to employ the aforementioned Discontinuous Galerkin methodology without any numerical issues. We have observed that in cases in which the viscoelastic response is significant (integer-order models or fractional models with α close to 1.0) and the relaxation times ratio $\frac{\tau_\epsilon}{\tau_\sigma}$ becomes too large, the scheme becomes unstable. In such cases, due to the explicit nature of our method, stability is only recovered by decreasing the time-step sufficiently so that it resolves the viscous time scale. Alternatively, this issue could be alleviated by using a total variation diminishing (TVD) implicit time integration scheme,[26] however at the expense of increased computational cost and implementation complexity.

Evaluation of Hereditary Integrals

A major computational challenge in considering viscoelastic models is posed by the need to evaluate the convolution integral in the expression for the viscoelastic pressure component, $p^V(t)$. This evaluation quantifies the stress–strain memory dependencies and needs to be repeated at every time step, and for every quadrature point of the domain. A naive implementation of this operation scales quadratically with the number of time steps, introducing a major computational bottleneck, both in terms of floating point operations and memory requirements. Here, we briefly present the methods and techniques we employed in this work to alleviate this issue and obtain a computable workflow.

Integer-Order SLS Model Following the approach of Steele *et al.*,[28] we explore the properties of the classic SLS exponential relaxation kernel and derive a simple updating rule that is independent of the time history imposed by the convolution operator.

$$I_{t+\Delta t}=\int_0^{t+\Delta t} e^{-\frac{(t+\Delta t-\gamma)}{\tau_\sigma}}p^{\mathrm{E}}(\gamma)d\gamma=e^{-\frac{\Delta t}{\tau_\sigma}}I_t+\int_t^{t+\Delta t} e^{-\frac{(t+\Delta t-\gamma)}{\tau_\sigma}}p^{\mathrm{E}}(\gamma)d\gamma, \tag{17}$$

where the last term corresponds to the time interval $[t,t+\Delta t]$ and can be computed using standard quadrature rules. This effectively allows us to consider the full history of the arterial wall response, without introducing any computational or memory bottleneck, as only the solution from the last time step needs to be stored.

Fractional-Order Models Due to the presence of power law (FO-Voigt model) or Mittag-Leffler (FO-SLS) relaxation kernels, fractional-order models do not admit the separability concept introduced above to obtain a simple updating rule for the hereditary integral. However, one can still avoid the "brute force" computation by appropriately choosing a smart algorithm. Here, we have employed the method developed by Lubich and Schädle.[15] Assuming that the convolution kernel is analytic for $t>0$ and locally integrable, López-Fernández *et al.*,[14] have proved that this method computes the convolution integral with spectral accuracy.

The key advantages of this algorithm is that it only requires $\mathcal{O}(n\log n)$ operations and $\mathcal{O}(n)$ memory, compared with the $\mathcal{O}(n^2)$ operations and memory

needed by a "brute force" approach for computing convolutions with n steps of history. Another advantage is that, for the FO-SLS model, we avoid the direct numerical approximation of the Mittag-Leffler function, and we only need to evaluate the Laplace transform of its derivative.[15]

We also report that in simulations where we adopted a "brute force" approach for computing Eq. (12), and directly evaluated the Mittag-Leffler function using the algorithm by Podlubny,[21] the solver suffered from instabilities triggered by errors in the approximation of the Mittag-Leffler function, with stability being recovered only when the function was approximated to very high accuracy. Since here we are interested in long-time integration of Eq. (1), direct approximation of the Mittag-Leffler function for long times and at the required level of accuracy is further problematic as it introduces a significant computational cost.

In the next section we present patient-specific simulation results of the 1D model in Eq. (1), coupled to purely elastic (Eq. (3)), and the SLS and FO-SLS (Eq. (12)) viscoelastic models. Integer- and fractional-order Voigt models are just limiting cases of the FO-SLS model and will be omitted from our attention in what follows.

RESULTS

Simulation Setup

All simulations were performed for a large patient-specific network that provides a detailed geometrical representation of the 50 largest arteries in the human brain, see Fig. 2. The data was obtained at the Department of Neurosurgery at Children's Hospital, Boston MA, USA. First, the 3D geometry was reconstructed from high-resolution magnetic resonance images (MRI) using an "in house" developed software package, and then, the 1D domain was extracted from the centerlines of the 3D vasculature. Consequently, the 1D representation considers arteries as straight tapering tubes, preserving the mean diameter and length of each of the 3D segments, while omitting curvature as well as bifurcation and junction branching angle information. The exact dimensions, model parameters and details of the reconstruction process for this network are given in Grinberg *et al.*[13]

Flow is driven from PC-MRI flowrate measurements at the four inlets (see Fig. 2): internal carotid (ICA) and vertebral (VA) arteries.[13] The 21 distal outlets are coupled to 3-element Windkessel models with parameters obtained from Grinberg *et al.*[13] Given the unavailability of pressure data measurements, these parameters are generally hard to estimate and may have a significant effect on the flow characteristics, leading to even incorrect results.[23] Here, we have observed that the chosen data set leads to low sensitivities and a physiologically correct solution for our case of interest (see Grinberg *et al.*[13]). The purely elastic response of the arterial wall is quantified by the β parameter, the values of which have also been taken from Grinberg *et al.*[13]

Regarding spatial discretization, the number of DG elements is primarily chosen with respect to the vessel's length. Mesh refinement is performed in regions of high flow gradients, with the final choice of the local polynomial order used (typically 3–8) resulting from mesh independence studies that ensure accurate resolution of the flow dynamics. Following Grinberg *et al.*,[13] we have a system with 200 degrees of freedom, and the computed solution does not depend on further resolution refinement. The initial conditions for all simulations are $(A, U)_{t=0} = (A_0, 0)$, and convergence to a periodic solution is obtained after two cardiac cycles. To ensure stability we have chosen a very small time-step $\Delta t = 6 \times 10^{-6} s$, a consequence of the high polynomial order that leads to a strict CFL condition and the viscoelastic dissipation introduced by the wall response. The computation of one cardiac cycle takes 30 s for elastic or integer-order viscoelastic models, and 15 min for fractional-order models (on a desktop with eight cores of Intel Xeon E5607@2.27 GHz).

Comparison of Integer- and Fractional-Order Viscoelastic Models

We have performed 1D blood flow simulations in the aforementioned cranial network using the integer order SLS, and the fractional order SLS pressure–area relation defined in Eqs. (12) and (13). The integer-order SLS pressure–area relation is determined by the triplet $\{\beta, \tau_\varepsilon, \tau_\sigma\}$, while, its fractional-order counterpart, is described by $\{\beta, \alpha, \tau_\varepsilon, \tau_\sigma\}$. The nature of these parameters is patient-specific and their values vary among anatomic locations, pathologies, age, *etc.*[3] Moreover, their accurate estimation in the clinical setting for various locations in an arterial network is a very challenging task. This leads to a very scarce selection of measured data in the literature, mostly corresponding to the aorta, the carotids and femoral arteries under *ex-vivo* or *in-vivo* conditions.

In this study, we have chosen four different relaxation time parameter sets from the literature, two for the integer order SLS and two for the fractional-order SLS model. The first set (model SLS1) corresponds to the estimations of Valdez-Jasso *et al.*,[29] where an integer-order SLS model was calibrated to fit measured data for the thoracic descending aorta and the carotid artery under *ex vivo* and *in vivo* conditions in ovine and

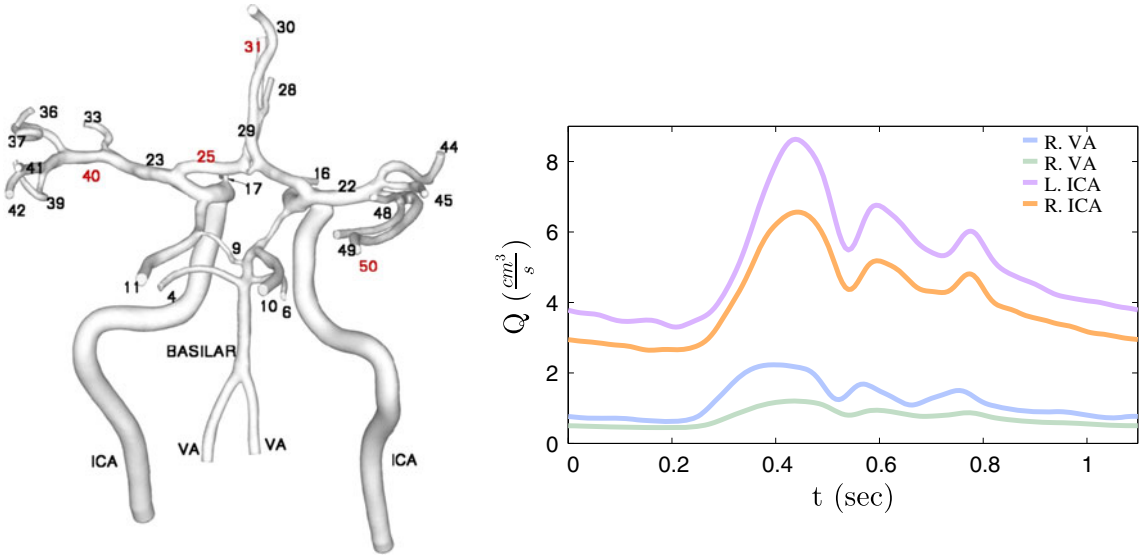

FIGURE 2. Left: Patient-specific cranial network from Grinberg *et al.*[13] Right: PC-MRI flowrate measurements at the four inlets (L. ICA, R. ICA, L. VA, R. VA).

TABLE 1. Viscoelastic model parameters.

Model	τ_ε (s)	τ_σ (s)	$\frac{\tau_\varepsilon}{\tau_\sigma}$	α
SLS1 (Valdez-Jasso *et al.*[29])	0.050	0.025	2.00	–
SLS2 (Lundkvist *et al.*[16])	29.3	16.9	1.49	–
FO-SLS1 (Doehring *et al.*[9])	1.84	0.076	24.12	0.29
FO-SLS2 (Craiem *et al.*[7])	11.74	7.61	1.54	0.20

human arteries. The second set (model SLS2) employs the parameters reported by Lundkvist *et al.*[16] for a healthy human femoral artery under *ex vivo* conditions. The third set (model FO-SLS1) is based on the measurements of Doehring *et al.*,[9] where a fractional-order SLS model was calibrated to *ex vivo* data for porcine aortic valve cusps. Finally, the fourth set (model FO-SLS2) corresponds to the mean values predicted by Craiem *et al.*[7] for a fractional-order SLS model fitted to *in-vivo* data from human ascending aorta segments. For comparison purposes we have also included the results obtained in Grinberg *et al.*[13] using the 1D model with a purely elastic pressure–area relation (model Elastic). Since our goal here is the comparison of different viscoelastic models, we have kept the same elasticity parameters reported in Grinberg *et al.*[13] for all cases considered. Table 1 summarizes the viscoelastic models we have employed in this section and their corresponding parameters.

In Figs. 3 and 4 we present the computed waveforms for flowrate and pressure as well as the pressure–area hysteresis loops due to viscoelastic dissipation at representative locations of the arterial network. We observe that all wall models except SLS2 lead to very similar flowrate wave propagation. However, with each model introducing a different amount of viscoelastic dissipation (see Fig. 4), the resulting local pressure waves present a variability up to 15%, although all models predict a very similar pressure drop between the inlets and the outlets. This is somewhat expected since the wall response is predominately elastic for all cases. The integer-order viscoelastic models correspond to a fractional order of $\alpha = 1.0$, yet a strong viscoelastic behavior is not observed due to the chosen relaxation times $\tau_\varepsilon \leq 2\tau_\sigma$ in both SLS1 and SLS2. Similarly, the relatively low values of the fractional order α in the FO-SLS1 and FO-SLS2 models leads to a dominant elastic response. Note, however, that the change in relaxation times from model SLS1 to SLS2 results to a significant change in the local pressure wave in each vessel (see Fig. 4), with the SLS2 model producing a stiffer response and predicting much smaller cross sectional wall displacements. This finding highlights the parametric sensitivity of the integer order SLS model: the discrete relaxation times $\{\tau_\varepsilon, \tau_\sigma\}$ dictate the viscoelastic wall response and strongly depend on the anatomic location. This dependence on the relaxation times introduces a caveat for using the integer order SLS model in simulations of large patient-specific arterial networks for which we only hope to have an estimate of τ_ε and τ_σ at few limited anatomic locations.

On the other hand, the behavior of the fractional models is dictated by the fractional order α which controls the interplay between elastic energy storage and viscoelastic dissipation. To better understand the role of α we red consider a FO-SLS model and vary the fractional order between $0 \leq \alpha \leq 1$ while keeping the same relaxation timescales with the SLS1 model: $\tau_\varepsilon = 0.050$ s and $\tau_\sigma = 0.025$ s. In Fig. 5 we present the

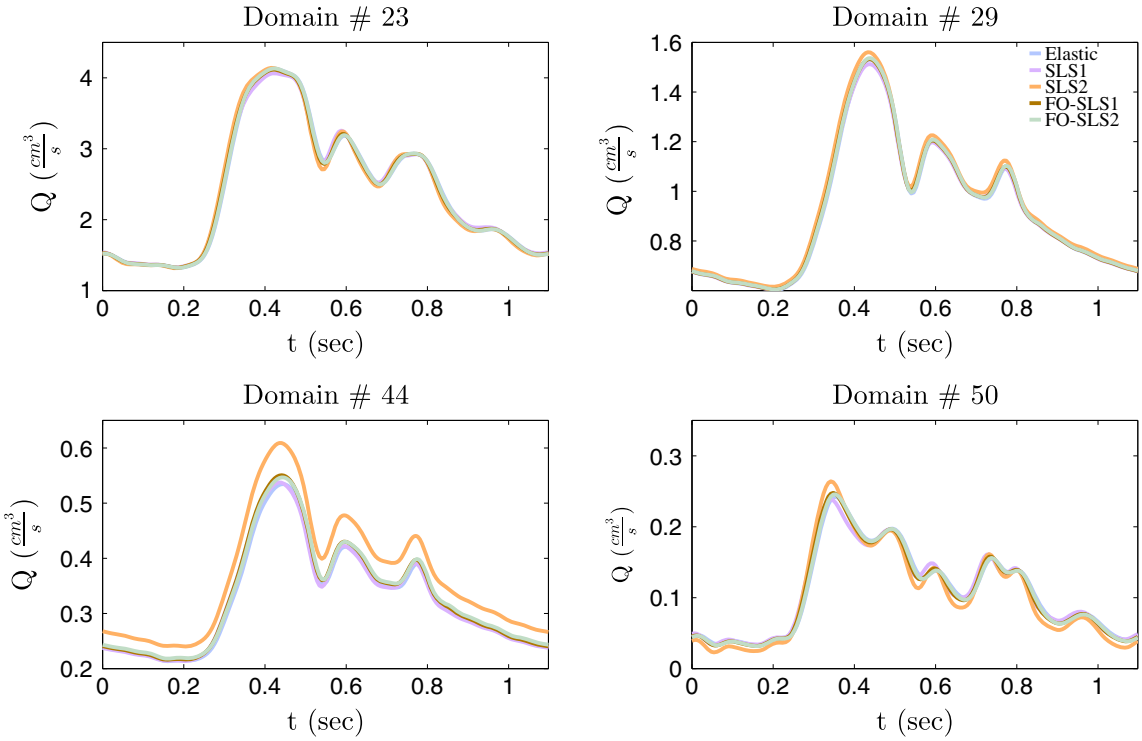

FIGURE 3. Comparison of the four viscoelastic model parameter sets in Table 1 over one cardiac cycle: Top left—computed flowrate at outlet # 23. Top right—computed flowrate at outlet # 29. Bottom left—computed flowrate at outlet # 44. Bottom right—computed flowrate at outlet # 50.

computed pressure wave at the left internal carotid artery (L. ICA) and the resulting pressure–area hysteresis loops for different values of α along with the purely elastic and integer order viscoelastic response. As expected, for $\alpha = 0$ we recover the purely elastic stress–strain response, while $\alpha = 1$ returns the solution of the integer order SLS1 model. For $\alpha \leq 0.5$ the response is predominately elastic and the solution is insensitive to the choice of relaxation times, with viscoelastic dissipation being only observed for large relaxation times ratio (see Fig. 4 for model FO-SLS1). Increasing the fractional order, the viscoelastic response becomes more important and the choice of relaxation times has a significant impact on the computed solution, both in terms of the pressure waveform and the amount of dissipation introduced in the system. This is illustrated in Fig. 5, where we have included results for the FO-SLS model with a larger relaxation time ratio $\frac{\tau_\epsilon}{\tau_\sigma} = 4$, while keeping the same short relaxation time $\tau_\sigma = 0.025$ s. This results to a pronounced viscoelastic response that noticeably affects the pressure wave propagation and the pressure–area hysteresis loops.

For $\alpha = 1.0$ the fractional-order SLS model reproduces the integer-order SLS model behavior and suffers from the same sensitivities. However, experimental studies in Craiem and Armentano,[5] Craiem *et al.*,[7] and Doehring *et al.*[9] suggest that $\alpha \approx 0.1 \div 0.3$ for larger systemic arteries, while they relate higher fractional orders to smooth muscle activation, which is a key flow auto-regulation agent in arteriolar networks. This may well indicate that muscular small arteries and arterioles exhibit higher fractional orders. Our simulations indicate that for $\alpha \in [0.0, 0.8]$, the effect of the FO-SLS model on the computed blood flow is primarily determined by the fractional order α with low sensitivity on the relaxation times ratio used.

Global Sensitivity Analysis of the Stochastic Fractional SLS Model

We consider a stochastic fractional order SLS model in which α, $\frac{\tau_\epsilon}{\tau_\sigma}$, and τ_σ are uniformly distributed random variables with value range taken from the literature: $\alpha \in [0, 1]$, $\frac{\tau_\epsilon}{\tau_\sigma} \in [1, 2]$, and $\tau_\sigma \in [0.02, 20.0]$. The corresponding three-dimensional parametric space is discretized with the probabilistic collocation method (PCM) on a tensor product grid generated by the nodes and weights of Legendre polynomials.[31] The number of collocation points per random dimension is 8, leading to a total of 512 sampling points. The simulation ran in parallel on 2048 cores of BG/Q, resulting to a total runtime of 1 h for three cardiac cycles.

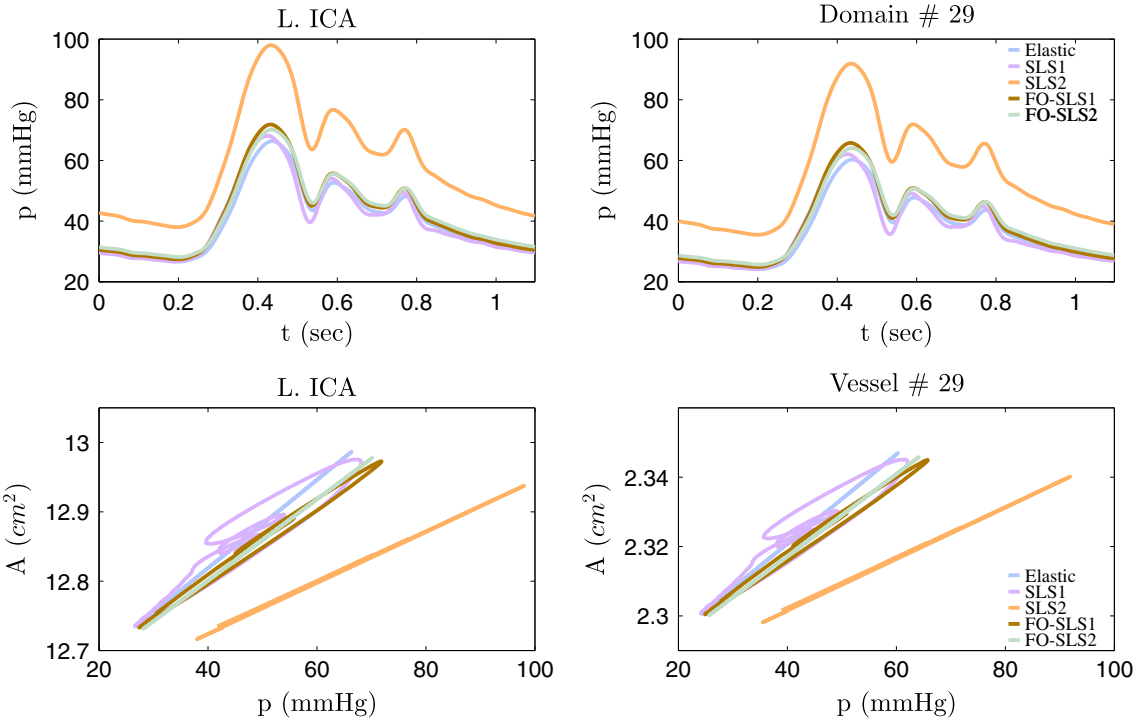

FIGURE 4. Comparison of the four viscoelastic model parameter sets in Table 1 over one cardiac cycle: Top left—computed pressure at one of the inlets (L. ICA). Top right—computed pressure at outlet # 29. Bottom left—computed pressure–area hysteresis loop at one of the inlets (L. ICA). Bottom right—computed pressure–area hysteresis loop at outlet # 29.

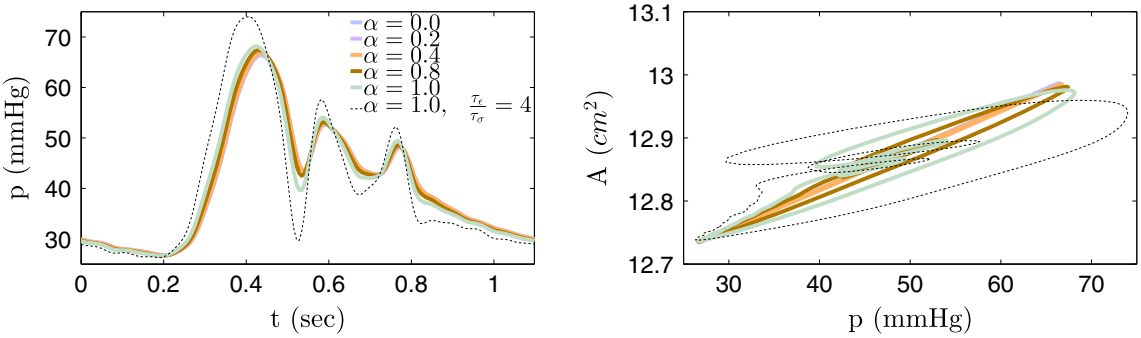

FIGURE 5. Computed pressure (left) and pressure–area hysteresis loop (right) at one of the inlets (L. ICA) for different values of the fractional order $0 \le \alpha \le 1$ and $\tau_\sigma = 0.025$ s, $\frac{\tau_\epsilon}{\tau_\sigma} = 2$. The dashed line corresponds to the integer-order model SLS1 (recovered for $\alpha = 1.0$) with a larger relaxation times ratio: $\tau_\sigma = 0.025$ s, $\frac{\tau_\epsilon}{\tau_\sigma} = 4$.

In Figs. 6 and 7 we present the computed mean flowrate and pressure wave ± 1 standard deviation for two representative locations in the network. The flowrate wave shows a deviation of less than 5% from the mean, indicating that wall viscoelasticity has a minor effect on its propagation. This fact is also in agreement with the results obtained when comparing the integer and fractional-order SLS models (Fig. 3). On the contrary, the pressure waveform displays significant variations primarily with respect to the fractional order α, but also with respect to the relaxation times ratio when $\alpha \to 1$ and the viscoelastic behavior is pronounced. This identifies the role of viscoelastic response as an agent that regulates pressure wave propagation by introducing viscoelastic energy dissipation. This effect is expected to be more pronounced in distal locations where arteries are more muscular and the associated fractional orders are high.

To further investigate the parametric sensitivity of pressure wave propagation on viscoelasticity we have performed a global stochastic sensitivity analysis study by computing the standard ANOVA decomposition[32] of the time-depended solution. Figure 8 shows the contribution of each random parameter and their second-order interactions to the total variance of the solution corresponding to the pressure at one of the

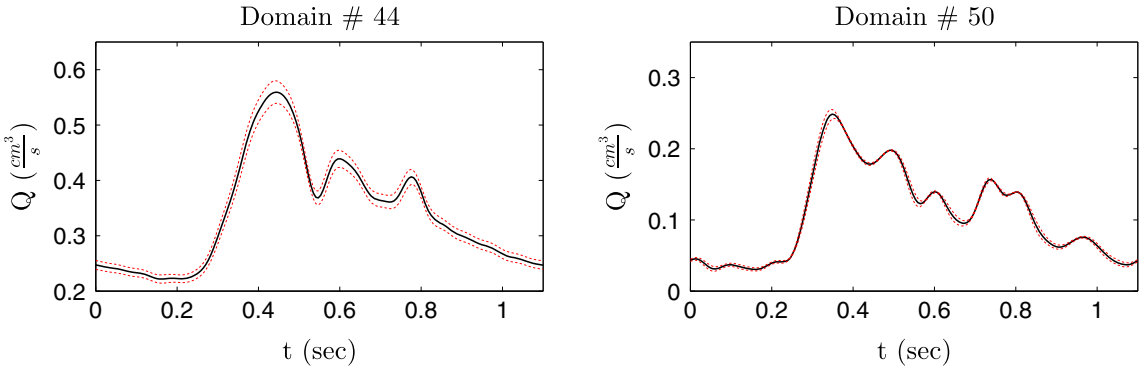

FIGURE 6. Stochastic fractional viscoelastic model simulations: computed mean flowrate (in black) and a variation of ± 1 standard deviation (in red) at different anatomic locations. Left: outlet # 44. Right: outlet # 50.

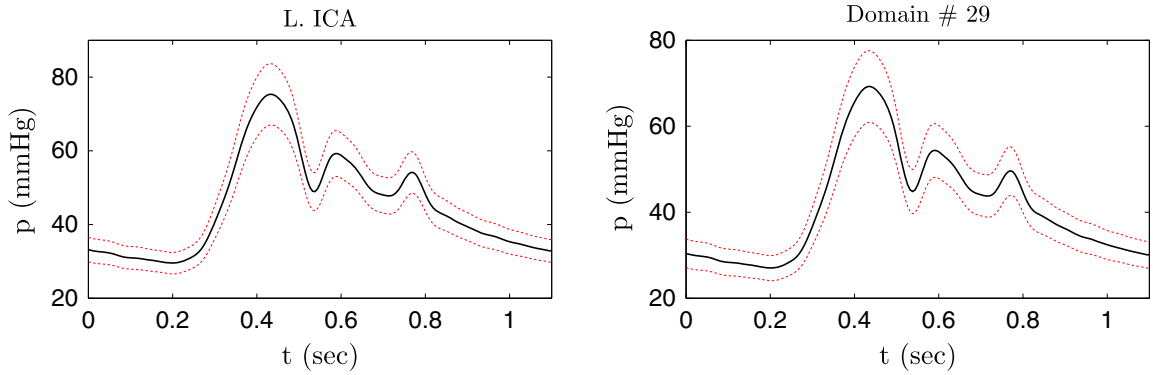

FIGURE 7. Stochastic fractional viscoelastic model simulations: computed mean pressure (in black) and a variation of ± 1 standard deviation (in red) at different anatomic locations. Left: inlet (L. ICA). Right: outlet # 29.

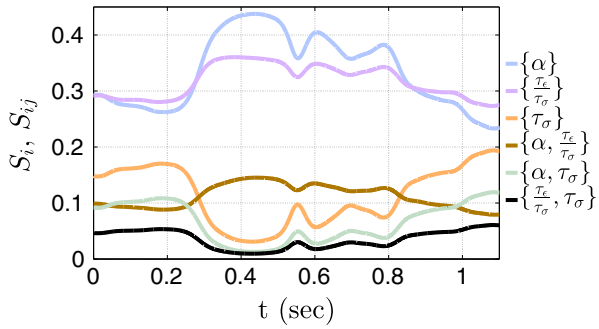

FIGURE 8. ANOVA global sensitivity analysis: variance decomposition of the computed pressure waveform at the inlet (L. ICA). S_i and S_{ij} are the global sensitivity indices of each random parameter and their pairwise interactions, respectively.

inlets (L. ICA). Clearly, the fractional order α is the most important parameter, with maximal influence during the systolic phase. This confirms the results presented in the previous sections, illustrating the effect of viscoelastic dissipation (introduced by increasing the fractional order) on the local pressure wave. The second most important parameter is the relaxation times ratio $\frac{\tau_\epsilon}{\tau_\sigma}$. In a similar fashion, a larger ratio introduces viscoelastic dissipation which, in turn, affects the local pressure, especially during the systolic phase. The opposite situation is observed for the short relaxation time τ_σ, as it only appears to have a noticeable variance contribution during the diastole. black Finally, Fig. 8 shows the variance contributions of pairwise interactions of the random parameters, indicating that their effect on the flow is less significant, especially during the systolic phase. We note that although these results are expected for the larger cranial arteries considered here, they provide a clear map of how arterial wall viscoelasticity affects hemodynamics.

DISCUSSION

We have performed deterministic and stochastic 1D blood flow simulations in a large patient-specific cranial network of compliant arteries corresponding to four different viscoelastic parameter sets. To this end, we have developed a fast parallel solver that supports integer and, for the first time, fractional wall models, enabling us to analyze in detail the effect of viscoelasticity on pulse wave propagation. black The solver can be made available to the community upon request and it is written in C++, employing the MPI and

OpenMP libraries to enable parallel, multithreaded processing.

First, we compared several models with the same elasticity parameters while the viscoelastic parameters are calibrated with data found in the literature. This comparison study indicated that all models lead to a similar flowrate wave propagation but the resulting local pressure waves are highly affected by the amount of viscoelastic dissipation introduced by each model. We observed that the viscoelastic behavior of integer-order models is strongly dependent on the choice of the relaxation times, while for fractional models, the response is dictated by the fractional-order. This fact makes fractional-order models very flexible as their conservative or dissipative nature is tuned by a single parameter, the fractional order α, while sensitivity of the solution to the relaxation parameters is only observed as $\alpha \to 1$. Consequently, fractional-order wall models provide a flexible tool, which may not only accurately capture the static response of the arterial wall but also, by dynamically tuning the fractional order α (which can be a function of time–space in fractional PDEs). One very interesting thrust for future work is neurovascular coupling, in which neural activity could be used to dynamically tune a variable-order fractional viscoelastic wall model model, accounting for smooth muscle activation effects that lead to vasodilation or vasoconstriction and provide a pressure auto-regulation mechanism.[30]

To further investigate the behavior of fractional viscoelastic models, a detailed uncertainty quantification study was performed. Using a stochastic wall model, we have computed a broad range of parametric combinations and reported the mean solution as well as the variabilities observed. We confirmed that wall viscoelasticity has only minor effects on flowrate wave propagation, while pressure waves and resulting wall displacements present variability in their phase and magnitude depending on the amount of viscoelastic dissipation introduced by the fractional order. Finally, by performing a global sensitivity analysis study, we have quantified the relative importance of the viscoelastic parameters and their second-order interactions throughout the span of a full cardiac cycle.

One of the limitations of the present work is that the viscoelastic behavior of each arterial wall model is defined by a single global set of viscoelastic parameters for all vessels. This is due the very limited availability of experimental results for most of the cranial arteries considered here. We believe that tuning the fractional-order locally for every segment will lead to a more concise modeling approach and we hope that future experimental studies will shed more light on how to appropriately choose it for different anatomic locations, pathologies, *etc*.

Finally, we must underline that validation is definitely the only path for accepting new tissue models, yet it still remains a very challenging task. In cases where local relaxation measurements are available, simple integer-order viscoelastic models can be calibrated to yield as good results as more general models with more relaxation timescales.[29] However, noninvasive parameter estimation becomes very hard for most distal anatomic locations, making these models suffer from high sensitivity to the relaxation timescales. These issues are key to the practical applicability of any model, and the main reason that may lead one to consider fractional-order models, leveraging on their better sensitivity properties and ability to model continuous relaxation at the expense of a single additional parameter, the fractional order α.

ACKNOWLEDGMENTS

This work was supported by the DOE Collaboratory on Mathematics for Mesoscopic Modeling of Materials (CM4), the NSF Directorate of Mathematical Sciences (DMS), and the DOE/INCITE program.

REFERENCES

[1]Alastruey, J., A. W. Khir, K. S. Matthys, P. Segers, S. J. Sherwin, P. R. Verdonck, K. H. Parker, and J. Peiró. Pulse wave propagation in a model human arterial network: assessment of 1-D visco-elastic simulations against in vitro measurements. *J. Biomech.* 44:2250–2258, 2011.

[2]Atanacković, T. M., S. Konjik, L. Oparnica, and D. Zorica. Thermodynamical restrictions and wave propagation for a class of fractional order viscoelastic rods. *Abstr. Appl. Anal.* 2011:1–32, 2011.

[3]Bia, D., I. Aguirre, Y. Zócalo, L. Devera, E. Cabrera Fischer, and R. L. Armentano. Regional differences in viscosity, elasticity, and wall buffering function in systemic arteries: pulse wave analysis of the arterial pressure–diameter relationship. *Rev. Esp. Cardiol. (Engl. Ed.)* 58:167–174, 2005.

[4]Čanić, S., C. J. Hartley, D. Rosenstrauch, J. Tambača, G. Guidoboni, and A. Mikelić. Blood flow in compliant arteries: an effective viscoelastic reduced model, numerics, and experimental validation. *Ann. Biomed. Eng.* 34(4): 575–592, 2006.

[5]Craiem, D. O., and R. L. Armentano. A fractional derivative model to describe arterial viscoelasticity. *Biorheology* 44:251–263, 2007.

[6]Craiem, D. O., F. J. Rojo, J. M. Atienza, R. L. Armentano, and G. V. Guinea. Fractional-order viscoelasticity applied to describe uniaxial stress relaxation of human arteries. *Phys. Med. Biol.* 53:4543, 2008.

[7]Craiem, D. O., F. J. Rojo, J. M. Atienza, G. V. Guinea, and R. L. Armentano. Fractional calculus applied to model arterial viscoelasticity. *Latin Am. Appl. Res.* 38: 141–145, 2008.
[8]DeVault, K., P. A. Gremaud, V. Novak, M. S. Olufsen, G. Vernieres, and P. Zhao. Blood flow in the circle of willis: modeling and calibration. *SIAM Multiscale Model. Simul.* 7(2):888–909, 2008.
[9]Doehring, T. C., A. D. Freed, E. O. Carew, I. Vesely, *et al.* Fractional order viscoelasticity of the aortic valve cusp: an alternative to quasilinear viscoelasticity. *J. Biomech. Eng.-Trans. ASME* 127:700, 2005.
[10]Eringen, A. C. Mechanics of Continua. Huntington, NY: Robert E. Krieger, 1980.
[11]Formaggia, L., A. Quarteroni, and A. Veneziani. Cardiovascular Mathematics: Modeling and Simulation of the Circulatory System, Vol. 1. New York: Springer, 2009.
[12]Fung, Y. Biomechanics: Mechanical Properties of Living Tissues. New York: Springer, 1993.
[13]Grinberg, L., E. Cheever, T. Anor, J. R. Madsen, and G. E. Karniadakis. Modeling blood flow circulation in intracranial arterial networks: a comparative 3D/1D simulation study. *Ann. Biomed. Eng.* 39:297–309, 2011.
[14]López-Fernández, M., C. Lubich, and A. Schädle. Adaptive, fast, and oblivious convolution in evolution equations with memory. *SIAM J. Sci. Comput.* 30:1015–1037, 2008.
[15]Lubich, C., and A. Schädle. Fast convolution for nonreflecting boundary conditions. *SIAM J. Sci. Comput.* 24:161–182, 2002.
[16]Lundkvist, A., E. Lilleodden, W. Siekhaus, J. Kinney, L. Pruitt, and M. Balooch. Viscoelastic properties of healthy human artery measured in saline solution by AFM-based indentation technique. In: *MRS Proceedings*, Vol. 436, 1996.
[17]Magin, R. L. Fractional Calculus in Bioengineering. Redding: Begell House, 2006.
[18]Mainardi, F. Fractional Calculus and Waves in Linear Viscoelasticity: An Introduction to Mathematical Models. London: Imperial College Press, 2010.
[19]Näsholm, S. P., and S. Holm. On a fractional Zener elastic wave equation. *Fract. Calc. Appl. Anal.* 16:26–50, 2013.
[20]Podlubny, I. Fractional Differential Equations, Vol. 198. San Diego: Academic Press, 1998.
[21]Podlubny, I. Calculation of the Mittag-Leffler function with desired accuracy. http://www.mathworks.com/matlabcentral/fileexchange/8738-mittag-leffler-function, 2012. Accessed 12 September 2012.
[22]Raghu, R., I. E. Vignon-Clementel, C. A. Figueroa, and C. A. Taylor. Comparative study of viscoelastic arterial wall models in nonlinear one-dimensional finite element simulations of blood flow. *J. Biomech. Eng.-Trans. ASME* 133(8):081003–081003, 2011.
[23]Reymond, P., F. Merenda, F. Perren, D. Rüfenacht, and N. Stergiopulos. Validation of a one-dimensional model of the systemic arterial tree. *Am. J. Physiol. Heart Circ. Physiol.* 297:208, 2009.
[24]Reymond, P., F. Perren, F. Lazeyras, and N. Stergiopulos. Patient-specific mean pressure drop in the systemic arterial tree, a comparison between 1-D and 3-D models. *J. Biomech.* 45(15):2499–2505, 2012.
[25]Sherwin, S. J., V. Franke, J. Peiro, and K. H. Parker. One-dimensional modelling of a vascular network in space–time variables. *J. Eng. Math.* 47:217–250, 2012.
[26]Shu, C. W. Total-variation-diminishing time discretizations. *SIAM J. Sci. Stat. Comput.* 9(6):1073–1084, 1988.
[27]Smith, N. P., A. J. Pullan, and P. J. Hunter. An anatomically based model of transient coronary blood flow in the heart. *SIAM J. Appl. Math.* 62:990–1018, 2001.
[28]Steele, B. N., D. Valdez-Jasso, M. A. Haider, and M. S. Olufsen. Predicting arterial flow and pressure dynamics using a 1D fluid dynamics model with a viscoelastic wall. *SIAM J. Appl. Math.* 71(4):1123–1143, 2011.
[29]Valdez-Jasso, D., D. Bia, Y. Zócalo, R. L. Armentano, M. Haider, and M. Olufsen. Linear and nonlinear viscoelastic modeling of aorta and carotid pressure–area dynamics under in vivo and ex vivo conditions. *Ann. Biomed. Eng.* 39(5):1–19, 2011.
[30]Witthoft, A., and G. E. Karniadakis. A bidirectional model for communication in the neurovascular unit. *J. Theor. Biol.* 311:80–93, 2012.
[31]Xiu, D., and D. E. Karniadakis. The Wiener–Askey polynomial chaos for stochastic differential equations. *SIAM J. Sci. Comput.* 24:619–644, 2002.
[32]Yang, X., M. Choi, G. Lin, and G. E. Karniadakis. Adaptive anova decomposition of stochastic incompressible and compressible flows. *J. Comput. Phys.* 231:1587–1614, 2012.